Microplastics and Nanoplastics

RESEARCH Open Access

Dynamics behavior of PE and PET oligomers in lipid bilayer simulations

Joni P. Järvenpää[1*] and Maija K. Lahtela-Kakkonen[1]

Abstract
In recent years many investigators have been concerned about the toxicity and potential health hazards of micro- and nanoplastics. However, we are still lacking a good understanding of the methods of their transport into the human body and subsequently within cells. This is especially true at the lower nanometer scale; these particles are potentially more dangerous than their micrometer counterparts due to their easier permeation into cells. In this study we used both unbiased molecular dynamics simulations and steered umbrella sampling simulations to explore the interactions of polyethylene terephthalate (PET) and polyethylene (PE) oligomers in phospholipid bilayers. Our simulations revealed that the bilayers did not represent significant energy barriers to the small oligomers; not only did they readily enter the cell membrane but they also became concentrated into specific parts of the membrane. The larger PET tetramers exhibited a strong aggregation in water but were the least likely to permeate through or into the membranes. It is possible that PE monomers and tetramers can become concentrated into membranes while PET monomers are more likely to pass through or concentrate just inside the membrane surface. Passive transport of microplastics into cells is, however, likely limited to particles of a few nanometers in diameter.

Keywords Microplastics, Nanoplastics, Membrane, Permeation, Molecular dynamics, Umbrella sampling

Introduction

Microplastics (MPs) are now a ubiquitous feature of the daily life of virtually all people in almost every part of the world [1–4]. In the past few years, as investigators have clarified the health risks of MPs, the general public is now rather well aware of the risks that they pose. MPs are usually considered to be plastic particles below 5 mm in diameter, although the lower limit is somewhat variable [1]. The 2022 WHO report suggested a lower limit of 1 μm with smaller particles i.e., those down to a limit of 1 nm to be called nanoplastics. Due to the ambiguity of naming MPs at the smallest nanometer level, we have applied the term oligomer here when describing plastic polymer chains that have a chain length from 1 to 100 monomer units. It has been reported that while MP particles less than 10 μm in size can be actively translocated into human tissues and exert effects on the immune response [1], passive transport is much more limited [5–7]. At sizes above 100 nm, passive permeation through membranes becomes much less probable. There is no clear cut-off point as the permeation depends on the properties of the particle and membrane in question. It seems that ease of permeation depends on multiple factors related to the particle i.e., its size, shape and surface properties as well as its possible charge or the presence of a corona. It has been suggested that particle sizes below 100 nm, especially those in the 1–10 nm range, could represent potential cell toxicity hazards as their cellular

*Correspondence:
Joni P. Järvenpää
joni.jarvenpaa@uef.fi
[1]School of Pharmacy, Faculty of Health Sciences, University of Eastern Finland, Kuopio 70210, Finland

intake is much more likely due to their propensity for passive diffusion. The potential health effects of MPs are still not well known, and research into the prevalence of these particles has been somewhat limited with respect to particles below 10 μm in size, although some toxicity testing has been conducted with sub-10 μm particles [1]. Truly comparable studies in the field are not available due to the lack of standardization and mismatches in particle sizes and properties between the reports in the literature [1, 4]. In addition, due to their relatively larger surface area, nanoplastics may carry more toxic chemicals and pollutants absorbed from the environment than a similar weight of larger MPs [8, 9]. The smallest nanoparticles have been less extensively investigated than their larger counterparts. PE has been found to trigger hepatic stress in fish, since due to its more hydrophobic nature, it has a tendency to absorb other hydrophobic pollutants [10].

Gastric fluid-system simulation studies have indicated that PET MPs can affect human gut microbiota communities and thus exert a negative effect on human health [11]. Nonetheless, the MP concentrations used in that study were based on very high daily exposures which were several orders of magnitude larger than those estimated by Mohamed Nor et al. (2021) [12]. This raises the question whether much more conservative MP concentrations would have appreciable adverse effects. Recently published studies have also detected MP fragments in human bloodstream and lungs [13, 14]. However, the study published by Leslie et al. (2022) [13] may potentially have suffered from significant contamination issues that may have affected the results, as suggested by Kuhlman (2022) [15]. These claims have not been supported or refuted by others; although the pattern of contamination points to possible external sources that had not been adequately addressed and the authors hypothesize an implausible inhomogeneity of the blood. Jenner et al. (2022) observed very large MP particles in lung tissue but it is questionable whether these sizes of particles would be able to reach this tissue. Contamination is a major issue in MP studies due to the prevalence of plastics in the laboratory and it is especially problematic in a surgical environment [16].

It not known how the MP's shape, surface properties, or the presence of a biomolecular corona determine their mechanism of ingestion and/or inhalation into the bloodstream; furthermore is it not clear whether there are strict size limits [17]. Mohamed Nor et al. (2022) estimated a global median intake of MP for adults as 583 ng/capita/day, although the intake can vary significantly depending on the food, water sources and country in question [12]. Several in vitro gut models have been used to study the effects of MPs in the gastro-intestinal tract with many different types of MP particles being tested [18]. The studies are unfortunately difficult to compare as they rarely share a standardized methodology, and the MP's particle properties and doses used vary significantly between reports making it difficult to conduct an accurate assessment of the outcomes of these trials on gut homeostasis.

The gastro-intestinal tract has an important gatekeeper role with respect to MP bioavailability. There are several possible mechanisms via which MPs can be taken up: (1) endocytosis (2) transcytosis through microfold cells (3) persorption (4) passive diffusion (5) active transport [17]. Large MP particles i.e., those with dimensions larger than >150 μm will be trapped within the intestinal mucus layer but they can make contacts with epithelial cells which may cause inflammation [19]. Smaller MPs, especially those below 1.5 μm, can be translocated through the mucus layer and reach the systemic bloodstream. However, only much smaller particles, those in the 1-100 nm range, are able to be passively transported through cell membranes [5, 7]. Permeability has been experimentally widely studied, for example, using the Caco-2 cell lines, since they differentiate spontaneously into cells possessing the morphology of small intestinal enterocytes [20]. The model does, however, have several limitations, i.e., it consists of only one type of cell with no mucus layer and there is a non-stirred water layer which does not mimic the condition in that tissue. This means that direct comparisons from these experiments to the in vivo situation are inadvisable.

In our previous study, single PE and PET monomers or tetramers showed a preference for specific parts of the membrane and the plastic oligomers were able to permeate the bilayer membranes in unbiased molecular dynamics simulations [21]. It is important to undertake molecular dynamics simulations of passive transport since they provide details into the structure–property relationships between taking into account the MP and via nanoplastic or oligomer chemistry one can apply passive-permeation thermodynamics to conduct high-throughput screening of multiple compounds. While in vitro and in vivo studies can provide some understandings of particle-membrane interactions in the highly complex cellular environment unfortunately, the cost and complexity of these tests limit high-throughput screening. Since MPs consist of vast numbers of different molecules, molecular dynamics (MD) of simple oligomers can help to select materials to be subjected to more specific or more extensive MD simulations or even experimental nano-scale permeability studies. For example, coarse-grained (CG) or umbrella sampling methods can be applied to simulate the permeation process of these kinds of molecules. Various hydrophobic compounds, such as octane and hexadecane and other hydrophobic compounds have been studied with the CG method; it has been found that lipid stability exerts a major impact on their properties [22].

In umbrella sampling, the molecule is pulled through the membrane and simulation windows are created along the pull coordinate, which allows sampling of even the more energetically unfavorable regions. This is especially useful when the energy barriers within a system, such as the lipid bilayers used here, impede an ergodic sampling. The umbrella sampling allows the energy landscape to be sampled as a molecule traverses across a membrane bilayer and one can calculate the potentials of mean force (PMF) [23]. When computing the PMF, umbrella sampling is considered to be one of the most reliable and is therefore a popular method. In addition to umbrella sampling, unbiased molecular dynamics simulations make it possible to study the free movement of multiple molecules, their interactions with each other and with the lipid bilayer structure as well as possible aggregation behaviors.

In this study we sought to investigate (1) the passive transport of common plastics through simplified membrane bilayers, (2) the atomic level interactions of the monomers and tetramers as well as (3) the molecular dynamics in a membrane system and (4) the feasibility of using MD for studying these properties by using both the umbrella sampling and unbiased simulation methods. We selected monomers and tetramers of polyethylene (PE) and polyethylene terephthalate (PET) which are the building blocks of the most commonly used plastics. Both compounds were considered to be small enough to plausibly permeate the membrane passively within the simulation time frames.

Materials and methods

We selected PE monomers (C_2H_4, MW: 28.05 g/mol), tetramers (C_8H_{18}, MW: 114.23 g/mol) and PET monomers ($C_{12}O_6H_{14}$, MW: 254.24 g/mol), tetramers ($C_{42}O_{18}H_{38}$, MW: 830.74 g/mol) for the molecular dynamics simulations with ethanol being used as a reference molecule. Bis(2-hydroxyethyl) terephthalate (BHET) was used as the monomer for PET. The molecular lengths in all-trans conformation were as follows: PE monomer: 0.25 nm, PE tetramer: 1.0 nm, PET monomer: 1.3 nm, PET tetramer: 4.5 nm CHARMM-GUI Ligand Reader & Modeler was used for generating the structure files for the small molecules [24]. The CHARMM General Force Field program was used for the ligand parameters [25, 26].

The membrane systems were built using the CHARMM-GUI Membrane Builder [27]. 128 Dipalmitoylphosphatidylcholine (DPPC) or 1-Palmitoyl-2-oleoylphosphatidylcholine (POPC) molecules were placed as a bilayer with TIP3P water model layers added on both sides. A total of 12 studied molecules were added to the system with four placed inside the membrane and sets of four on either side of the membrane on the outside. The molecules were placed at 10 Å intervals in X, Y directions and 40 Å in the Z direction (Fig. S1). Bilayers with no added small molecules were also constructed as reference membranes. Water molecules within 2 Å from the added molecules were removed using the VMD molecular graphics viewer (version 1.9.3) in order to avoid clashes in the early minimization and equilibration runs [28].

Gromacs version 2019.4 was used for the simulations with a CHARMM36m force field [29]. The system was equilibrated similarly as in our previous study [21]. The system was briefly equilibrated for 1 ns in the NVT ensemble followed by 1 ns in NPT at 2 fs time steps. No restraints were used on the studied small molecules in equilibration runs as precise starting locations were not needed. For the production runs in NPT ensemble, the Nose-Hoover thermostat was used with temperatures of 323 K for DPPC and 310 K for the POPC membranes and the Parrinello-Rahman barostat for the pressure. Three replication runs were carried out, each run lasting 100 ns. Periodic boundary conditions were applied. Various Gromacs tools were used when analyzing the results.

In the umbrella sampling simulations, single molecules were used starting in the water phase, at a distance of 40 Å for most molecules. A 50 Å translation was used for the much larger PET tetramer to prevent any overlap with the membrane before simulation. The molecules were pulled towards the center of mass of all phosphorus atoms on the opposite side of the membrane bilayer with a force constant of 500 kJ/mol·nm^2 and a speed of 5 nm per ns. A total of 50 configurations were created along the pull coordinate. Data from the center of the bilayer towards the phosphorus atoms on the other side were calculated and seen to be symmetrical. Each generated configuration was then equilibrated for 1 ns and afterwards run in the NPT ensemble for 10 ns. Instead, 20 ns was used for the larger PET tetramer as testing at 10 ns was found not to be adequate. Other molecules showed no discernible differences between 10 and 20 ns. The Weighted Histogram Analysis Method (WHAM) was used to obtain the potentials of mean force (PMF) from the 10 ns runs with the values being presented as means [30]. The umbrella histograms were analyzed to confirm that there was sufficient overlap to permit proper sampling. The first and last 0.2 nm of the PMF profiles were cut out and the new start point set at 0 to remove spiking of the energy profile at its endpoints due to poor sampling.

Results and discussion

Initially we used unbiased molecular dynamics simulations to examine the free movement of 12 inserted monomers or tetramers of either PE or PET in DPPC and POPC membranes. Ethanol was used as a small reference molecule in the membranes. In previous research, ethanol has been demonstrated by Carpenter et al. (2014)

and Ghorbani et al. (2020) to easily permeate lipid bilayers, especially those present in POPC and DOPC [31, 32]. Because of this, and its rough structural similarities with the monomers, we selected it as a reference compound. Interactions between the molecules and their behavior in the system were assessed by a combination of visual inspection, counting which approximate frames molecules were in close contact, and assessing hydrogen bond counts per frame for the hydrophilic molecules and partial density graphs.

Ethanol was readily capable of entering or exiting the membrane and moved quickly in both directions i.e., inside and back through the membrane. Nonetheless, it slightly preferred to stay in the aqueous phase and avoided the center of the membrane (Fig. 1). Ethanol displayed a greater preference to stay inside in POPC membranes than with the DPPC counterparts. No aggregation was seen for ethanol and hydrogen bonding occurred very rarely with other ethanol molecules. The changes in the area per lipid or bilayer thickness of the bilayer were insignificant (around 0.5% difference to pure DPPC or POPC membranes). Thus, significant changes to the properties of the membrane caused by alcohols are likely only visible when much higher concentrations are present, as found by Pinisetty et al. (2006) and Gupta et al. (2020) [33, 34]. Ethanol's maximum density peak was found to be inside the membrane close to the phosphorus density peak, with two minima at the center of the bilayer and at the phosphorus density peak, where it was seen to form hydrogen bonds with the headgroups. Ethanol's overall behavior was almost identical to that described in our previous study [21].

PE monomers behaved very similarly to ethanol, since they are also small molecules, i.e., they were able to move around easily and quickly in the water and move inside the membrane as found in our previous study [21]. The monomers of PE evidently preferred to locate inside the membrane where they were able to move more freely (Fig. 2). This finding is in agreement with the more hydrophobic nature of PE as compared to the polar molecule ethanol; a clear difference was seen despite the very small size (0.25 nm) of the PE monomers. No aggregation behavior or significant changes to area per lipid or bilayer thickness of the bilayer were evident (only up to 1% difference to pure DPPC or POPC membrane). There was no clear difference between PE's preference for the membranes of DPPCs or POPCs. The maximum density peak for PE was observed to be at the center of the bilayer, with the minima close to the two phosphorus density peaks.

PE tetramers underwent some slight aggregation behavior in both aqueous and membrane phases, mostly as pairs of molecules. They also clearly preferred the membrane, more so than the PE monomer (Fig. 3A). Movement into the membrane was rarer than with monomers, but once inside, they stayed there consistently and became concentrated over time. Instead, it was very rare that they returned to the aqueous phase. Their speed of movement was not significantly different from the monomers. Area per lipid rose very slightly as compared with the monomer, while the thickness of the bilayer remained the same (around 1% changes to pure membrane for both values). The POPC system had on average 2–3 more molecules inside the membrane at the end of the simulation than were present in the DPPC

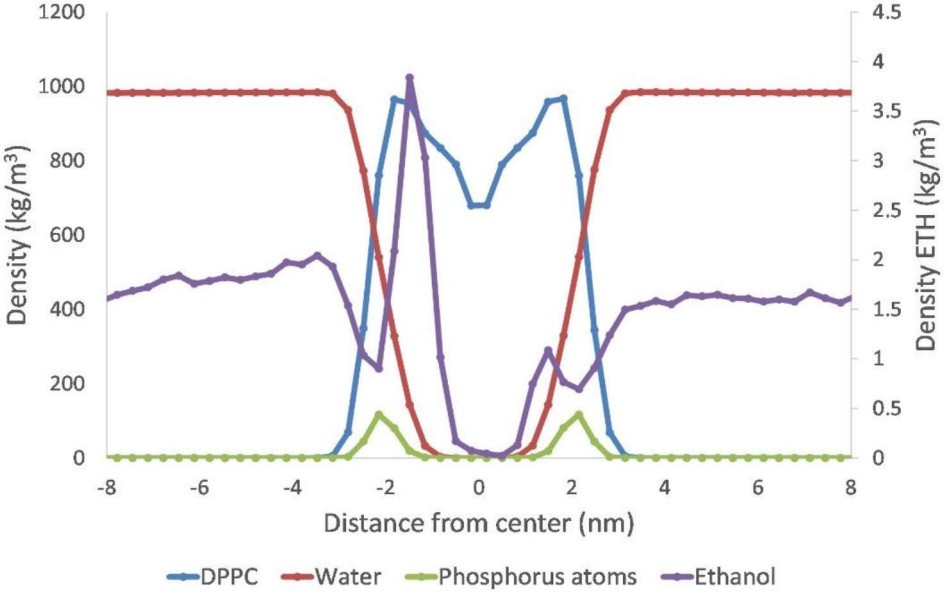

Fig. 1 Mass density profile of an ethanol simulation in the DPPC membrane. Ethanol prefers to become located in the inside of membrane close the phosphorus density peaks, similarly to PET.

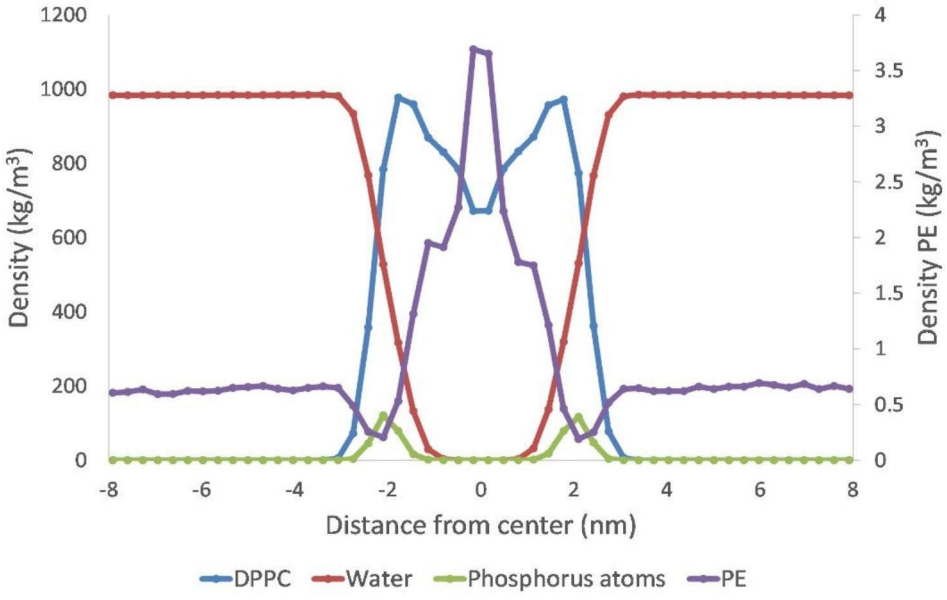

Fig. 2 Mass density profile of a PE monomer simulation in DPPC membrane. PE prefers the center of the bilayer

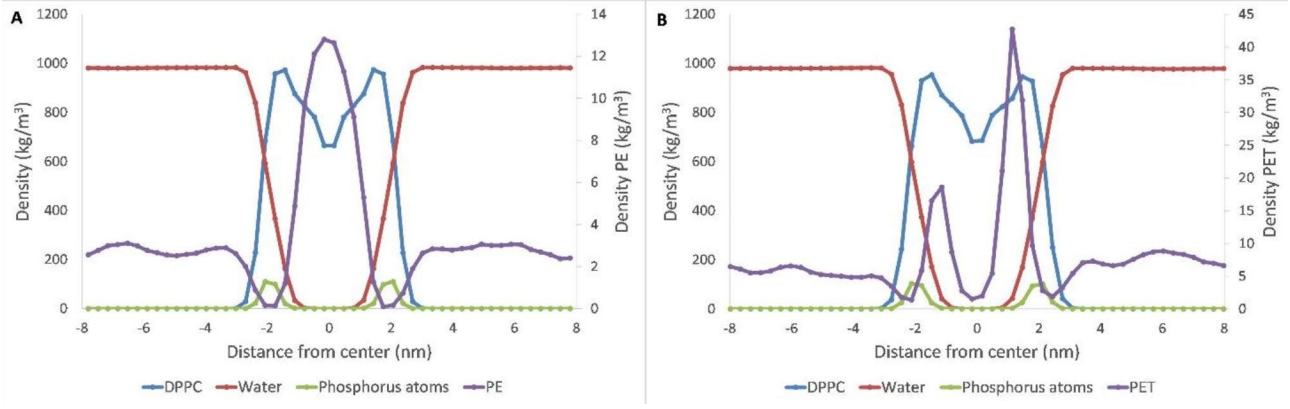

Fig. 3 Mass density profile of (**A**) PE tetramer simulation in DPPC membrane shows that PE clearly prefers to be located within the symmetrical center of membrane with some movement in the aqueous phase while (**B**) the PET monomer prefers to locate in the inside of membrane close to the phosphorus density peaks

setup. The maximum density peak was at the center of the membrane with density minima at the phosphorus density peaks. The minima peaks were more pronounced than with the monomer. The concentration of PE monomers and tetramers at the bilayer center was similar to that observed by MacCallum and Tieleman (2006), which is not surprising given their lipophilic nature [35]. Experimentally PE present in MP has been studied in cell membranes obtained from human colorectal Caco-2 cells. Unfortunately, the results are somewhat contradictory since Gautam et al. (2022), [36] reported decreased cell viability after exposure while in the publication from Stock et al. (2021) [37], no effect was observed. In an in vivo study conducted by Li et al. (2020) [38], mice fed with MP containing PE particles (10–150 μm) showed higher histological scores than their reference animals. However, it should be noted that both Gautam et al. (2022) and Li et al. (2020) used considerably larger MP particles which would not passively permeate through membranes. Unfortunately, very short-chain plastic oligomers have not been studied either in vitro or in vivo, complicating comparisons to the results obtained with MD. Course-grained simulations with small hydrophobic molecules, including octane (PE tetramer), have been carried out previously by Barnoud et al. (2014) and Orsi et al. (2009) [22, 39]; both groups detected major changes in the stability of lipid membranes caused by significant concentrations of hydrophobic molecules. Furthermore, the aliphatic molecules preferred the interface region between the headgroups and tail groups, findings resembling those reported here. This location was seen to have the greatest effect on membrane stability as at that

site, the molecules could act as linactants at rather low concentrations.

The PET monomers were occasionally able to enter the membrane. Their movement and preferred locations in the membrane were similar to that observed for ethanol, although PET moved more slowly with a stronger preference to stay inside the membrane (Fig. 3B). There was some aggregation behavior, although it was significantly more extensive and longer lasting than observed with PE tetramers. The hydrogen bonds between the PET monomers were also far more common than in the simulations undertaken with ethanol. Aggregation outside the membrane was mostly in pairs, although occasionally several molecules appeared to aggregate into a group interacting along the hydrophobic areas with their hydrophobic groups turned towards the center of the aggregate. Inside the membrane, the hydrophilic areas and hydrogen bonding were favored with respect to the interactions. A pair of monomers could also interact with each other's hydrophilic hydroxyl groups and form a perpendicular line through the membrane with opposite ends of the pair forming hydrogen bonds with the headgroups on each side of the bilayer. This was, however, rare as the monomers seemed to prefer to locate closer to the membrane surface and stay mostly horizontal to the membrane. In addition, horizontally interacting molecules were formed at the density peak areas close to the membrane surface, as seen in Fig. 3B. The interactions with other molecules could aid the molecule either when entering or when exiting the membrane. These interactions close to the surface could also allow one end of a molecule to partially exit the membrane while the other interacting molecules tended to anchor the aggregate within the membrane (Fig. 4A-C). The overall movement was slower than with ethanol or PE e.g., movement into the membrane was also much slower, which is not surprising considering PET's larger size. In POPC membranes, the PET molecules showed more movement through the membrane surface than in the DPPC membranes where movement across the surface was rare. The PET compounds caused slightly more pronounced changes to the bilayer structure than was evident with PE. An increase was seen in the area per lipid (~2%) and a more significant (+3%) drop in bilayer thickness. The density peaks were present on both sides of the bilayers at just below the phosphorus peaks, similarly to the situation with ethanol. Roughly equal density minima were at the phosphorus peaks and the bilayer center, unlike ethanol which had a less pronounced minima at the phosphorus peak. Chen et al. (2016) noted that bisphenol A, a molecule that shares structural similarities with the PET monomer showed very similar behavior as observed in our study [40], although bisphenol A did display aggregation behavior which resembled more the PET tetramer rather than the monomer.

The PET tetramers did not enter or exit the membrane. In the aqueous phase, they quickly underwent intense aggregation into dense stable spheroids of up to 2–3 nm in size within the first few nanoseconds of the simulations, growing larger over time (Fig. S2). The movement of the larger tetramers was less erratic than that of the monomers, being slowed by this significant aggregation behavior. Inside the membrane, the tetramers aggregated much less and were found to be more loosely side by side, similarly to the monomers (Fig. S3). The interactions inside the membrane occurred mostly through the polar groups, lasting for much shorter times than the aggregates in water. The molecules formed L- and Z- shapes inside the membrane, as observed in our

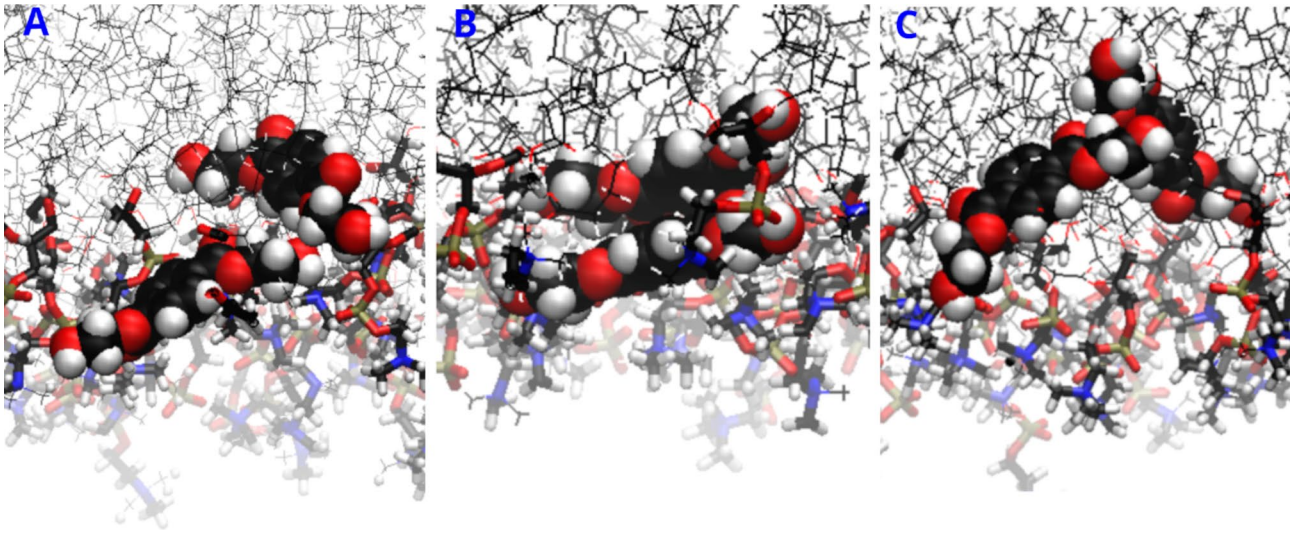

Fig. 4 PET assisted permeation through the membrane's surface. (**A**) Two PET molecules interact at the membrane's surface through hydrogen bonding. (**B**) Both molecules move inside the membrane. (**C**) Molecules become detached and remain inside the membrane

previous study [21]. In some simulations, a single PET tetramer would turn on one side of the membrane for a few nanoseconds while the others kept their perpendicular orientations within the membrane. Movement inside the membrane was slow and they tended to stay in groups that were rather close to each other. Hydrogen bond formation between PET molecules in the water phase and the membrane headgroups did occur occasionally, although interactions between the PET inside and outside were very rare. The behavior of the PET tetramers in POPC and DPPC membranes was very similar i.e., their density inside the bilayer was at a maximum on both sides of the center, with the exact center slightly lower and the phosphorus density peaks close to zero. Unlike all other molecules, which had very average density distributions across the aqueous layer, the density in water was seen to be skewed into quite large peaks in one or two locations (Fig. 5). This was caused by the aggregation of PET into one or two aggregates rather rapidly during the simulations, which did not move extensively after their formation. The thickness of the bilayer did not change noticeably, instead the area per lipid grew most significantly at 2.5% for DPPC and 3.5% for POPC of all molecules.

Changes in the thickness of the bilayer over time were analyzed for all molecules. No significant changes were evident on average across the whole length of the simulation when compared to pure membranes for any molecule. The area per lipid did not vary extensively, however, there were more pronounced changes as the molecule size became greater, with PET tetramers exhibiting the largest changes. As movement of these molecules into the membrane did not take place in unbiased simulations, it is unclear whether they exerted any effect on the molecule's propensity to enter or exit the membrane. It is likely that more significant changes would be possible if much larger amounts or longer oligomers per lipid were present in the systems as shown by Hollóczki and Gehrke (2020) [41], where clearer differences were observed.

The temperature for the DPPC membrane system was set 13 K higher than the POPC due to the gel transition temperature being lower [42]. Due to this temperature difference, it is inadvisable to directly compare the findings from the DPPC and POPC simulations. In all simulations, the bilayer structure remained intact, which was confirmed by deuterium order parameter calculations (Fig. S4-S15), partial density graphs and visual inspection. The traversing of the test molecules or ethanol did not cause any significant effects in comparison to the pure DPPC or POPC membranes as seen from the order parameters, area per lipid and bilayer thickness. The behavior and preferred location in the membranes in unbiased simulations with 12 added molecules exhibited similarities as found in our previous study, which concentrated on single molecules [21]. Thus, the addition of multiple molecules, or taking into account their aggregation behavior did not seem to exert significant effects on their interactions with the membranes.

The umbrella sampling technique was applied to study the permeation energies and obtain the PMF. The studied molecules were pulled from the water phase towards the phosphorus atoms on the opposite side of the membrane bilayer (Fig. 6A-C). A total of 50 configurations were created along the pull coordinates, which after a 1

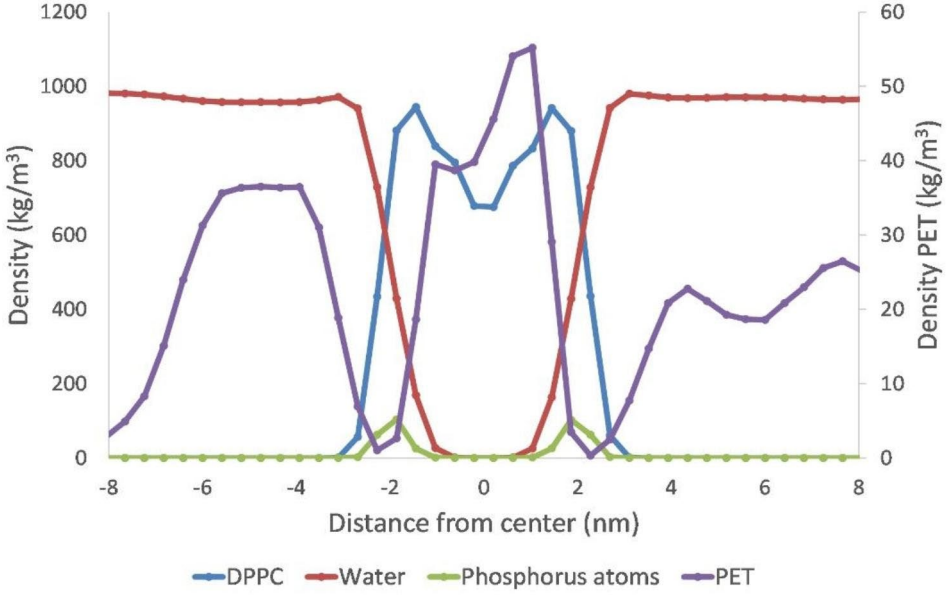

Fig. 5 Mass density profile of a PET tetramer in a simulation in DPPC membranes. The distribution in water is non-uniform due to the formation of slow-moving PET aggregates

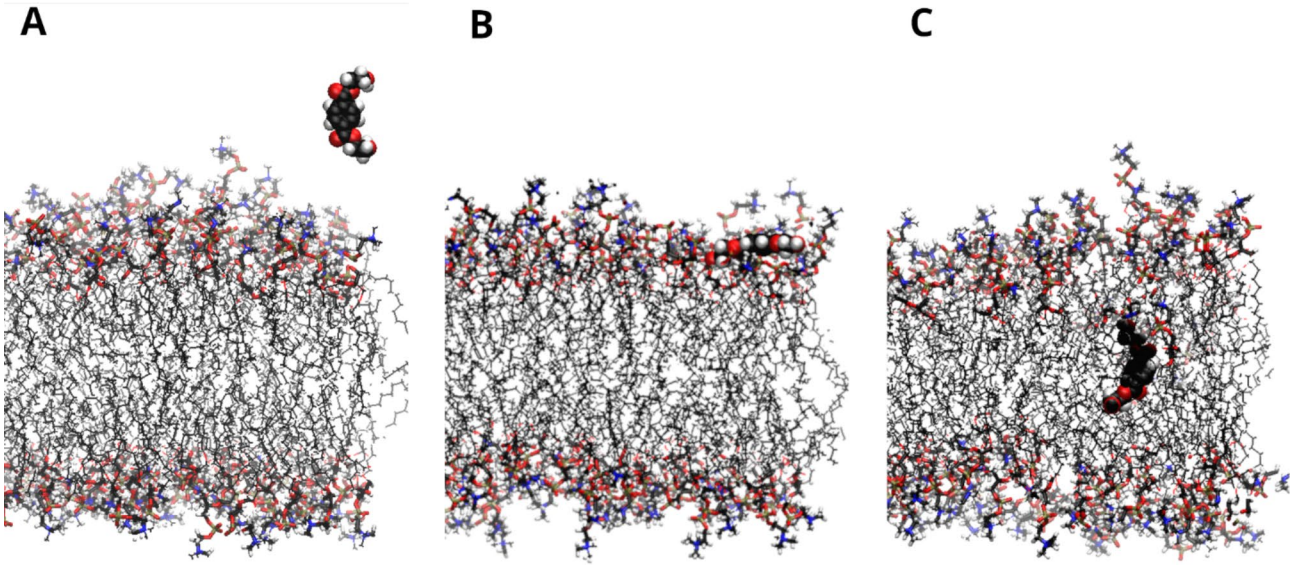

Fig. 6 Umbrella sampling process. An example of a PET monomer that has been pulled from the aqueous phase into the membrane. (**A**) PET is in solution (water not visible), (**B**) PET is at the membrane surface and (**C**) has moved into the membrane. The necessary sampling windows were created along the route that the molecules were pulled

Table 1 Umbrella sampling PMF values (kcal/mol) presented as the mean from three replicate simulations for membrane center barrier (ΔG_m), lipid headgroups barrier (ΔG_b) and energy minima inside membrane (ΔG_{min}) shown for both membranes

Molecule	DPPC			POPC		
	ΔG_m	ΔG_b	ΔG_{min}	ΔG_m	ΔG_b	ΔG_{min}
Ethanol	3.4	0.7	0.1	2.1	0.4	-0.4
PE monomer	-1.4	1.1	-1.4	-1.3	0.9	-1.3
PE tetramer	-6.3	1.1	-6.3	-7.5	0.7	-7.5
PET monomer	5.1	1.8	-0.1	5.3	1.4	-0.1
PET tetramer	5.9/10.5	4.4	2.0	10.3/15.5	2.8	-0.1

ns NPT equilibration, were then simulated for 10 ns each. The WHAM tool was used to obtain the PMF values (Table 1).

For ethanol, the calculated free energy changes from the aqueous phase, which was set at 0, to the membrane center (ΔG_m) were 3.4 kcal/mol for DPPC and 2.1 kcal/mol for POPC (Fig. 7). Additionally, an initial barrier for the lipid headgroups region (ΔG_b) was calculated as 0.7 kcal/mol for DPPC and 0.4 kcal/mol for POPC. The initial barrier is a typical phenomenon as the solute interacts with the headgroups region [43], and this was seen in all simulations. The energy minimum was set at below the phosphorus density peak that was close to the equal energy to water for DPPC (0.1 kcal/mol) and slightly below it for POPC (-0.4 kcal/mol). This likely explains why in the unbiased simulations, ethanol preferred to stay more inside the POPC membranes than in the corresponding DPPCs. POPC membranes consistently exhibited lower barriers for both the initial headgroups as well as the bilayer center in almost all simulations for the other studied molecules as well. DPPC and POPC membranes have not been extensively compared, but Frallicciardi et al. (2022) also consistently observed higher permeability of various polar solutes in POPC membranes than in DPPC membranes [44]. In both cell membranes, ethanol was still easily able to enter or exit the membrane and move around within the membrane rapidly; the low energy barriers calculated in umbrella sampling simulations confirm the results obtained from the unbiased simulation. Our results showed similar free-energy profiles to the values described previously for ethanol [32, 34].

The PE monomer presented an initial barrier at the headgroups' region that was slightly higher than ethanol with ΔG_b of 1.1 kcal/mol for DPPC and 0.9 kcal/mol for POPC (Fig. 8). The center of the bilayer was at a lower energy level than the starting point of water with the minima at the very center with ΔG_m of -1.4 kcal/mol for DPPC and −1.3 kcal/mol for the POPC membranes. Smaller local minima were also visible at both sides of the center, at a distance of roughly 1 nm where the density peaks for the lipid tails were located. The values of

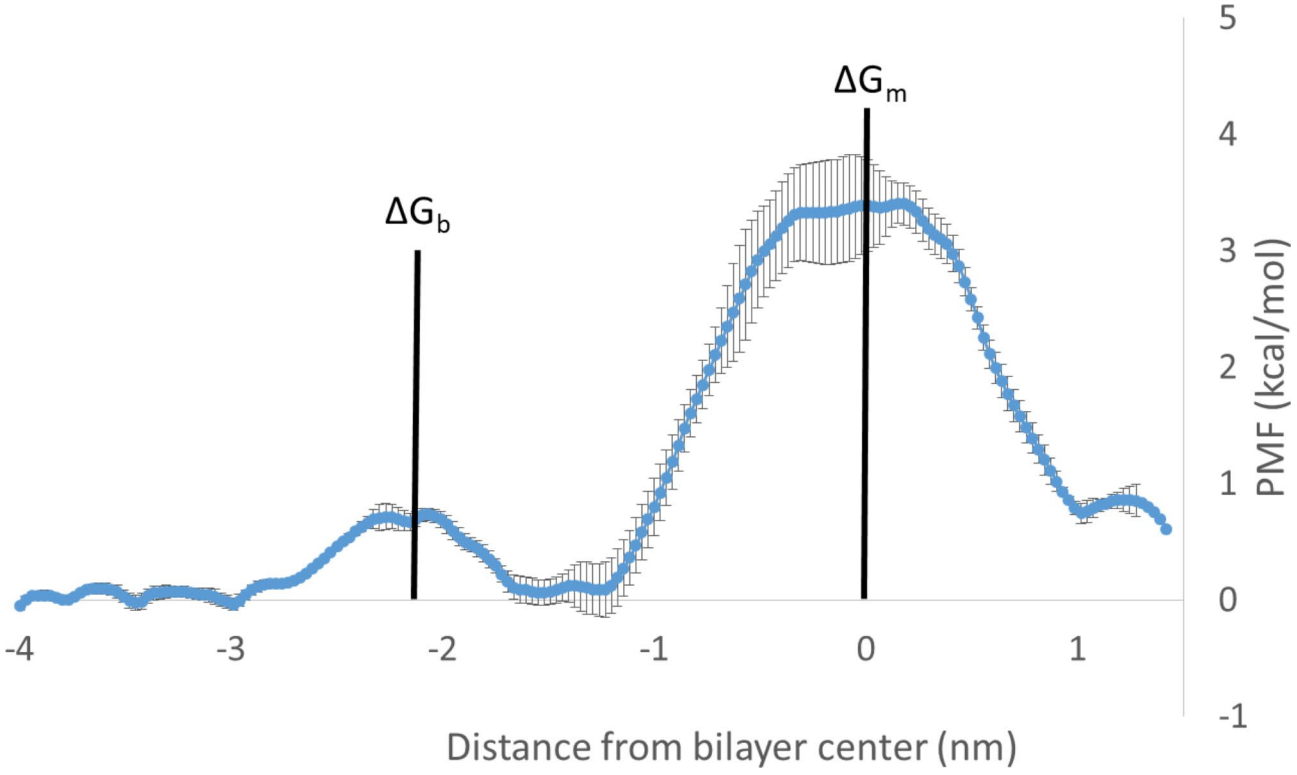

Fig. 7 Mean (SD) of PMF of three consecutive replicate umbrella sampling simulations with ethanol in a DPPC bilayer. The initial headgroups barrier (ΔG_b) can be seen at just over 2 nm from the center (ΔG_m)

ΔG_m were not significantly small, making it likely that transport through the bilayer was rather straightforward without there being any significant concentration into any part of the membrane. This was also seen in the unbiased simulations where PE was able to easily move inside the membrane. The more hydrophobic nature of the PE monomers, as compared to ethanol, likely explains the slightly higher initial barrier energies at the polar headgroups region, as well as the lower energies at the bilayer center. Interestingly, the PE tetramers had almost identical initial barrier energies as assessed by ΔG_b as the monomers. The parallel orientation of the PE with the bilayer lipids during entry could affect this phenomenon. The hydrophobic interior of the membrane possibly lowered the entry energies as the further end of the molecule started interacting with the interior, counteracting the larger size of the tetramer which otherwise would have had slightly higher barrier energies than the monomer. The PET molecules did not exhibit a similar behavior.

The PE tetramer possessed very similar headgroup barrier energies as the monomer with ΔG_b of 1.1 kcal/mol for DPPC and 0.7 kcal/mol for POPC (Fig. 9). The center of the bilayer displayed a much lower energy level, however, with the values of ΔG_m as -6.3 kcal/mol for DPPC and −7.5 kcal/mol for POPC. The exact center of the bilayer was similar in energy as the region with the tailgroups; also no local minima close to the center were seen as had been noted with the monomer. As the center of the bilayer was at a much lower energy level for the tetramer than for the monomer, it seems likely that it is more likely that the tetramer could become concentrated inside the membrane. Likewise in unbiased simulations, the tetramer showed a greater preference than the monomer to stay inside the membrane.

The PET monomer showed similarities to ethanol with an energy minimum at just inside the phosphorus density peak, which was very slightly below the starting energy levels in water with −0.1 kcal/mol for both DPPC and POPC (Fig. 9B). The bilayer center was visible as a slightly lower energy region than that where the lipid tails were located. The headgroups and bilayer center barriers were, however, significantly higher for PET than ethanol with the values of ΔG_m of 5.1 kcal/mol for DPPC and 5.3 kcal/mol for POPC and ΔG_b of 1.8 kcal/mol for DPPC and 1.4 kcal/mol for POPC.

The PET tetramer encountered a strong barrier at the center of the membrane with ΔG_m of 5.9 kcal/mol for DPPC and 10.3 kcal/mol for POPC (Fig. 10). The initial barrier ΔG_b for DPPC at 4.4 kcal/mol was also quite large, however the POPC barrier was much lower, only 2.8 kcal/mol. Both membranes displayed significant energy minima for the tetramers just below the surface, i.e., at 2.0 kcal/mol for DPPC and −0.1 kcal/mol for POPC.

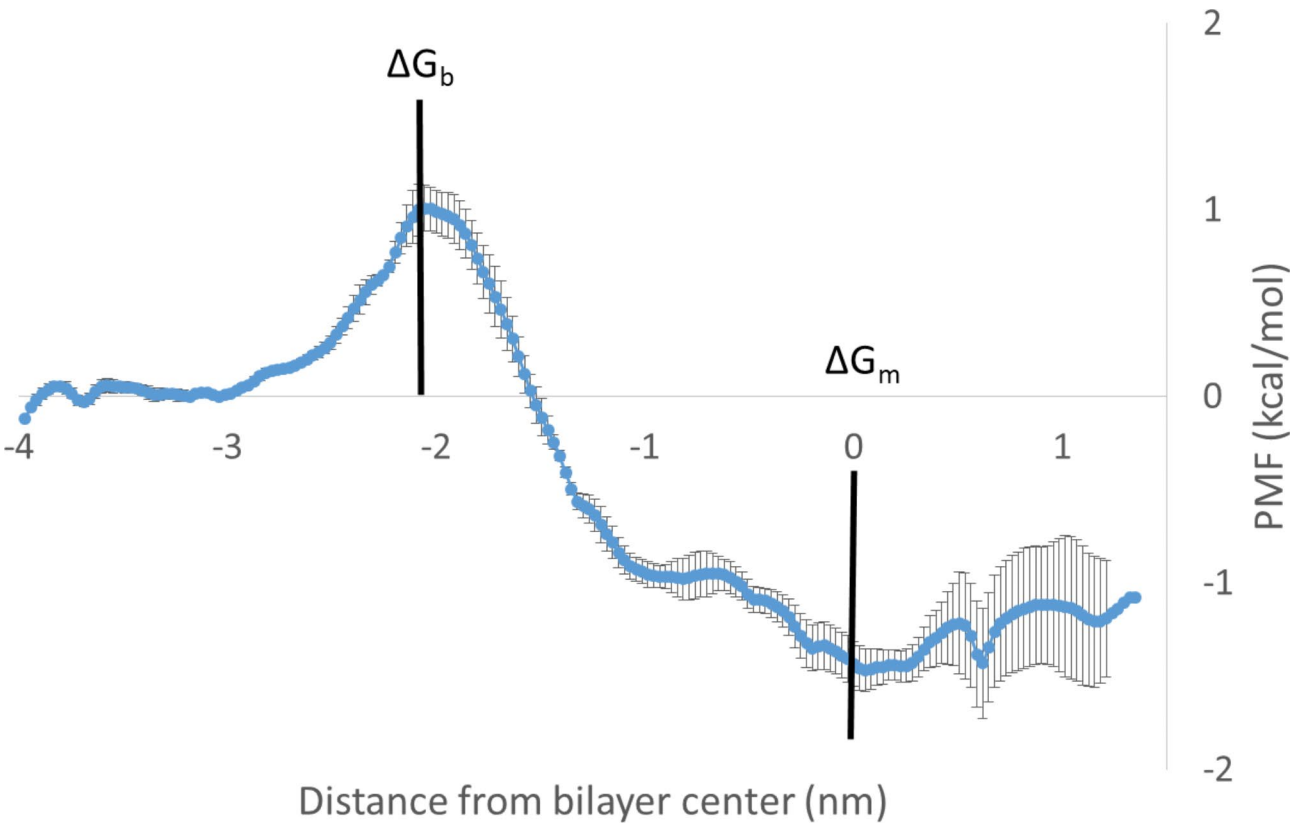

Fig. 8 Mean (SD) of PMF figure of three consecutive replicate umbrella sampling simulations of PE monomer in DPPC bilayer. The initial headgroups barrier (ΔG_b) can be seen at just over 2 nm from the center (ΔG_m)

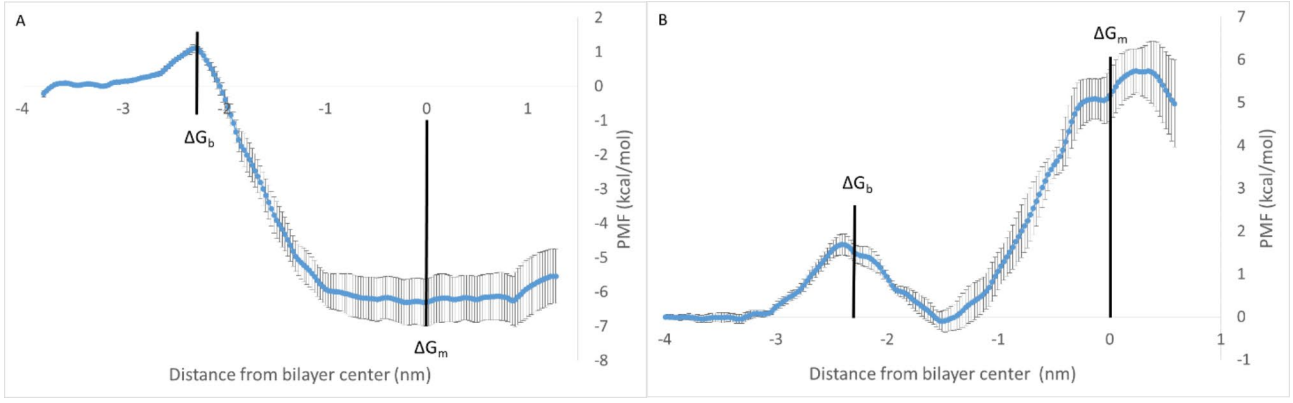

Fig. 9 Mean (SD) of PMF of three consecutive replicate umbrella sampling simulations of (**A**) PE tetramer or (**B**) PET monomer in DPPC bilayer. The initial headgroups barrier (ΔG_b) can be seen at just over 2 nm from the center (ΔG_m)

This might explain why in the unbiased simulations, a single PET tetramer was able to partially shift close to the membrane surface into this region for a short time. The energies did not level out in the simulations, as the very long molecules had not completely traversed inside the membrane by the end of simulation when the other end touched the lipid's phosphorus atoms on the opposite bilayer leaflet. Both the DPPC membrane (10.5 kcal/mol) and the POPC (15 kcal/mol) reached significantly higher energies at the end of the simulation. It would likely be preferable in future studies investigating larger hydrophobic oligomers to initially allow a molecule to seek a preferred shape in water in an unbiased molecular dynamics simulation and only after the preferred shape has been reached then to conduct a steered simulation by pulling the molecule into the membrane. There would still be a significant issue of randomness in the orientation, but that might be corrected by testing various different orientations.

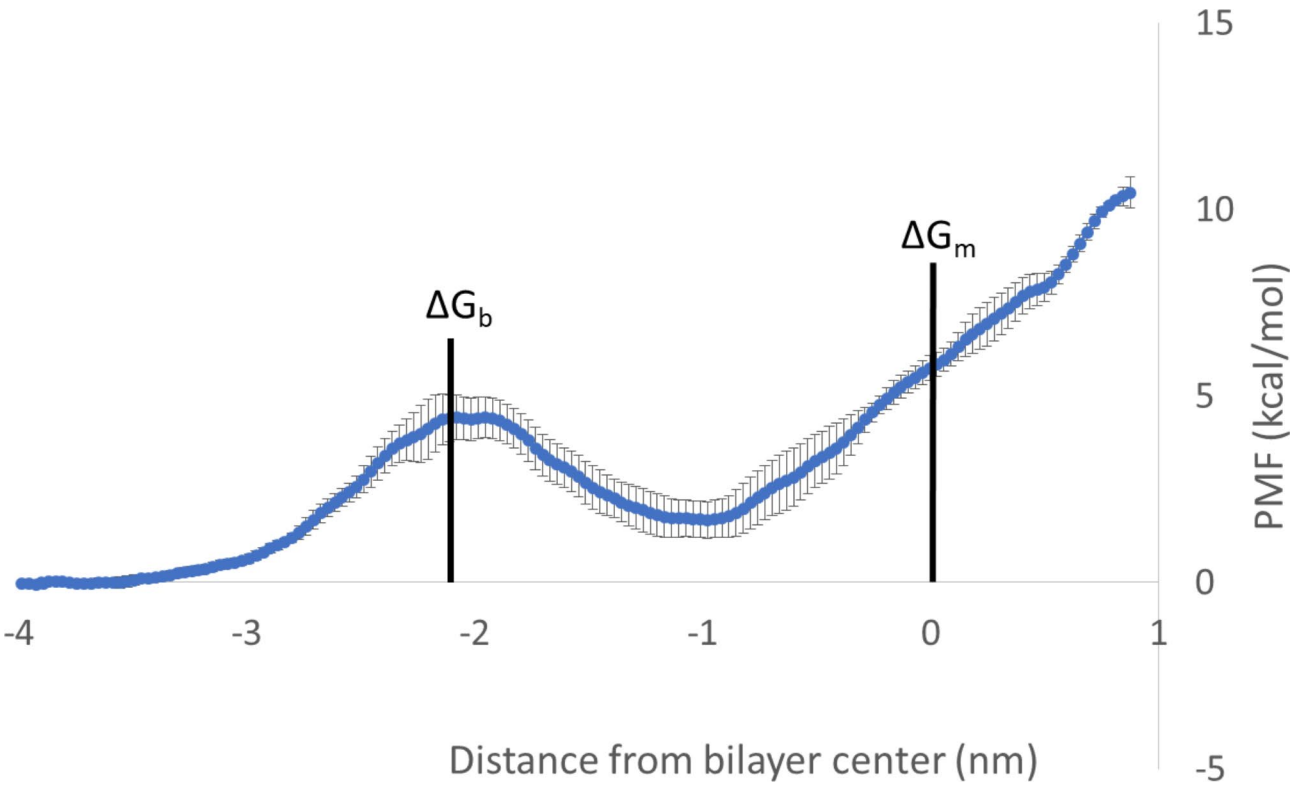

Fig. 10 Mean (SD) of PMF figure of three consecutive replicate umbrella sampling simulations of PET tetramer in the DPPC bilayer. The initial headgroups barrier (ΔG_b) can be seen at just below 2 nm from the center (ΔG_m)

Conclusions

Both the unbiased and steered simulations revealed that the monomers and PE tetramers were easily transported through the bilayer surface. PE, especially its tetramers, was more likely to concentrate in the membrane. The POPC bilayers showed slightly lower thresholds than DPPC. The effects of the molecules on the bilayer structure were not significant. Since passive transport seems to be limited to molecules in the nanometer size-range, simulation studies can be especially beneficial in clarifying their transport mechanisms. The transport of micro- or nanoplastics across membranes is still in its infancy; this is a topic that needs to be investigated in the future since the effects and possible toxicity of micro- and nanoplastics on human health are unknown. Nonetheless, it is very difficult to compare experimental results with different MPs since they are dependent on the molecule's type, size and shape as well as on the treatment conditions. Similarly, it is inadvisable to compare molecular modeling studies of MPs which have used different methods, e.g., CG to all-atom. Nonetheless a better understanding concerning the passive-permeation properties of oligomers and polymers would be beneficial when evaluating the health effects of these compounds. This phenomenon needs to be clarified at an atomic scale before studying the larger systems of MPs. We have demonstrated that small oligomers can readily cross lipid membranes without exerting any significant effects on the membrane's structure. The chemical structure of the monomers influences their behavior in lipid membranes. It will be necessary to gain a better understanding of the permeation mechanisms of oligomers into cells at the atomic level before scaling-up the simulations into particle permeation experiments with larger MPs. Based on our findings, scaling-up the oligomers should not require extensive parameter refinement when conducting MD, but it is recommended that larger oligomer chains would benefit from initial minimization in water before inserting them into a system as this initial minimization would allow for a more natural starting point for the larger molecules.

Abbreviations

PET	Polyethylene terephthalate
PE	Polyethylene
MP	Microplastic
MD	Molecular dynamics
CG	Coarse-grained
PMF	Potential of mean force
BHET	Bis(2-hydroxyethyl) terephthalate
DPPC	Dipalmitoylphosphatidylcholine
POPC	1-Palmitoyl-2-oleoylphosphatidylcholine
WHAM	Weighted Histogram Analysis Method
ΔGm	Membrane center barrier
ΔGb	Lipid headgroups barrier
ΔGmin	Energy minima inside membrane
SD	Standard deviation

Supplementary Information

The online version contains supplementary material available at https://doi.org/10.1186/s43591-023-00076-0.

Supplementary Material 1

Acknowledgements
The authors thank the CSC-IT Center of Science Limited for providing software and computational resources and Ewen McDonald (PhD) for proofreading the manuscript. This work was supported by the Drug Research Doctoral Program at University of Eastern Finland.

Author contributions
All authors conceived and designed the study, conducted experiments and analyzed the results and contributed to the writing of the manuscript. All authors reviewed and approved the final version of manuscript.

Funding
This work was supported by the University of Eastern Finland doctoral school.

Data Availability
The datasets generated and/or analyzed during the study are available from the corresponding author on reasonable request.

Declarations

Ethics approval and consent to participate
Not applicable.

Consent for publication
Not applicable.

Competing interests
The authors declare no competing interests.

Received: 23 May 2023 / Accepted: 21 November 2023
Published online: 01 December 2023

References

1. Dietary. and Inhalation exposure to nano- and microplastic particles and potential implications for human health. Geneva: World Health Organization; 2022.
2. Yang X, Man YB, Wong MH, Owen RB, Chow KL. Environmental health impacts of microplastics exposure on structural organization levels in the human body. Sci Total Environ. 2022;825:154025. https://doi.org/10.1016/j.scitotenv.2022.154025.
3. Koelmans AA, Diepens NJ, Mohamed Nor NH. (2022) Weight of Evidence for the Microplastic Vector Effect in the Context of Chemical Risk Assessment. In: Bank MS, editor. Microplastic in the Environment: Pattern and Process. Environmental Contamination Remediation and Management: Springer Open. 1 ed. p. 155 – 97. https://doi.org/10.1007/978-3-030-78627-4_6.
4. Kirstein IV, Gomiero A, Vollertsen J. Microplastic pollution in drinking water. Curr Opin Toxicol. 2021;28:70–5. https://doi.org/10.1016/j.cotox.2021.09.003.
5. Smith DJ, Leal LG, Mitragotri S, Shell MS. Nanoparticle transport across model cellular membranes: when do solubility-diffusion models break down? J Phys D: Appl Phys. 2018;51:294004. https://doi.org/10.1088/1361-6463/aacac9.
6. Shang L, Nienhaus K, Nienhaus GU. Engineered nanoparticles interacting with cells: size matters. J Nanobiotechnol. 2014;12:5. https://doi.org/10.1186/1477-3155-12-5.
7. Pye CR, Hewitt WM, Schwochert J, Haddad TD, Townsend CE, Etienne L, Lao Y, Limberakis C, Furukawa A, Mathiowetz AM, Price DA, Liras S, Lokey RS. Nonclassical size dependence of Permeation defines Bounds for Passive Adsorption of large drug molecules. J Med Chem. 2017;60(5):1665–72. https://doi.org/10.1021/acs.jmedchem.6b01483.
8. Geiser M, Rothen-Rutishauser B, Kapp N, Schürch S, Kreyling W, Schulz H, Semmler M, Im Hof V, Heyder J, Gehr P. Ultrafine particles cross cellular membranes by nonphagocytic mechanisms in lungs and in cultured cells. Environ Health Perspect. 2005;113(11):1555–60. https://doi.org/10.1289/ehp.8006.
9. Gigault J, El Hadri H, Nguyen B, Grassl B, Rowenczyk L, Tufenkji N, Feng S, Wiesner M. Nanoplastics are neither microplastics nor engineered nanoparticles. Nat Nanotechnol. 2021;16(5):501–7. https://doi.org/10.1038/s41565-021-00886-4.
10. Smith M, Love DC, Rochman CM, Neff RA. Microplastics in Seafood and the Implications for Human Health. Curr Environ Health Rep. 2018;5(3):375–86. https://doi.org/10.1007/s40572-018-0206-z.
11. Tamargo A, Molinero N, Reinosa JJ, Alcolea-Rodriguez V, Portela R, Bañares MA, Fernández JF, Moreno-Arribas MV. PET microplastics affect human gut microbiota communities during simulated gastrointestinal digestion, first evidence of plausible polymer biodegradation during human digestion. Sci Rep. 2022;12(1):528. https://doi.org/10.1038/s41598-021-04489-w.
12. Mohamed Nor NH, Kooi M, Diepens NJ, Koelmans AA. Lifetime Accumulation of Microplastic in children and adults. Environ Sci Technol. 2021;55(8):5084–96. https://doi.org/10.1021/acs.est.0c07384.
13. Leslie HA, van Velzen MJM, Brandsma SH, Vethaak AD, Garcia-Vallejo JJ, Lamoree MH. Discovery and quantification of plastic particle pollution in human blood. Environ Int. 2022;163:107199. https://doi.org/10.1016/j.envint.2022.107199.
14. Jenner LC, Rotchell JM, Bennett RT, Cowen M, Tentzeris V, Sadofsky LR. Detection of microplastics in human lung tissue using μFTIR spectroscopy. Sci Total Environ. 2022;831:154907. https://doi.org/10.1016/j.scitotenv.2022.154907.
15. Kuhlman RL. Letter to the editor, discovery and quantification of plastic particle pollution in human blood. Environ Int. 2022;167:107400.
16. Field DT, Green JL, Bennett R, Jenner LC, Sadofsky LR, Chapman E, et al. Microplastics in the surgical environment. Environ Int. 2022;170:107630. https://doi.org/10.1016/j.envint.2022.107630.
17. Zhao SA. Summary of the transporting mechanism of Microplastics in Marine Food Chain and its effects to humans. IOP Conf Ser Earth Environ Sci. 2022;1011:012051.
18. Fournier E, Etienne-Mesmin L, Grootaert C, Jelsbak L, Syberg K, Blanquet-Diot S, Mercier-Bonin M. Microplastics in the human digestive environment: a focus on the potential and challenges facing in vitro gut model development. J Hazard Mater. 2021;415:125632. https://doi.org/10.1016/j.jhazmat.2021.125632.
19. EFSA. Presence of microplastics and nanoplastics in food, with particular focus on seafood. EFSA J. 2016;14(6):e04501. https://doi.org/10.2903/j.efsa.2016.4501.
20. Lea T. Caco-2 cell line. In: Verhoeckx K, Cotter P, López-Expósito I, Kleiveland C, Lea T, Mackie A, Requena T, Swiatecka D, Wichers H, editors. The Impact of Food Bioactives on Health: in vitro and ex vivo models [Internet]. The Impact of Food Bioactives on Health. Volume 2. Cham: Springer; 2015. pp. 103–11. https://doi.org/10.1007/978-3-319-16104-4_10.
21. Järvenpää J, Perkkiö M, Laitinen R, Lahtela-Kakkonen M. PE and PET oligomers' interplay with membrane bilayers. Sci Rep. 2022;12(1):2234. https://doi.org/10.1038/s41598-022-06217-4.
22. Barnoud J, Rossi G, Marrink SJ, Monticelli L. Hydrophobic compounds reshape membrane domains. PLoS Comput Biol. 2014;10(10):e1003873. https://doi.org/10.1371/journal.pcbi.1003873.
23. You W, Tang Z, Chang CA. Potential Mean Force from Umbrella Sampling simulations: what can we learn and what is missed? J Chem Theory Comput. 2019;15(4):2433–43. https://doi.org/10.1021/acs.jctc.8b01142.
24. Kim S, Lee J, Jo S, Brooks CL 3rd, Lee HS, Im W. CHARMM-GUI ligand reader and modeler for CHARMM force field generation of small molecules. J Comput Chem. 2017;38(21):1879–86. https://doi.org/10.1002/jcc.24829.
25. Vanommeslaeghe K, Hatcher E, Acharya C, Kundu S, Zhong S, Shim J, Darian E, Guvench O, Lopes P, Vorobyov I, Mackerell AD Jr. CHARMM General Force Field: A Force field for Drug-Like molecules Compatible with the CHARMM all-Atom Additive Biological Force Field. J Comput Chem. 2010;31(4):671–90. https://doi.org/10.1002/jcc.21367.
26. Yu W, He X, Vanommeslaeghe K, MacKerell AD Jr. Extension of the CHARMM General Force Field to Sulfonyl-Containing compounds and its utility in Biomolecular simulations. J Comput Chem. 2012;33(31):2451–68. https://doi.org/10.1002/jcc.23067.
27. Jo S, Kim T, Iyer VG, Im W. CHARMM-GUI: a web-based graphical user interface for CHARMM. J Comput Chem. 2008;29(11):1859–65. https://doi.org/10.1002/jcc.20945.
28. Humphrey W, Dalke A, Schulten K. VMD: visual Molecular Dynamics. J Mol Graph. 1996;14(1):33–8. https://doi.org/10.1016/0263-7855(96)00018-5.
29. Abraham MJ, Murtola T, Schulz R, Páll S, Smith JC, Hess B, Lindahl E. GROMACS: high performance molecular simulations through multi-level parallelism from laptops to supercomputers. SoftwareX. 2015;1:19–25. https://doi.org/10.1016/j.softx.2015.06.001.

30. Hub JS, de Groot BL, van der Spoel D. g_wham—A free weighted histogram analysis implementation including robust error and Autocorrelation estimates. J Chem Theory Comput. 2010;6(12):3713–20. https://doi.org/10.1021/ct100494z.
31. Carpenter TS, Kirshner DA, Lau EY, Wong SE, Nilmeier JP, Lightstone FC. A method to predict blood-brain barrier permeability of drug-like compounds using molecular dynamics simulations. Biophys J. 2014;107(3):630–41. https://doi.org/10.1016/j.bpj.2014.06.024.
32. Ghorbani M, Wang E, Krämer A, Klauda JB. Molecular dynamics simulations of ethanol permeation through single and double-lipid bilayers. J Chem Phys. 2020;153(12):125101. https://doi.org/10.1063/5.0013430.
33. Pinisetty D, Moldovan D, Devireddy R. The effect of methanol on lipid bilayers: an atomistic investigation. Ann Biomed Eng. 2006;34(9):1442–51. https://doi.org/10.1007/s10439-006-9148-y.
34. Gupta R, Badhe Y, Rai B, Mitragotri S. Molecular mechanism of the skin permeation enhancing effect of ethanol: a molecular dynamics study. RSC Adv. 2020;10(21):12234–48. https://doi.org/10.1039/d0ra01692f.
35. MacCallum JL, Tieleman DP. Computer Simulation of the distribution of hexane in a lipid bilayer: spatially resolved Free Energy, Entropy, and Enthalpy profiles. J Am Chem Soc. 2006;128(1):125–30. https://doi.org/10.1021/ja0535099.
36. Gautam R, Jo J, Acharya M, Maharjan A, Lee D, PB KC, Kim C, Kim K, Kim H, Heo Y. Evaluation of potential toxicity of polyethylene microplastics on human derived cell lines. Sci Total Environ. 2022;838(Pt 2):156089. https://doi.org/10.1016/j.scitotenv.2022.156089.
37. Stock V, Laurisch C, Franke J, Dönmez MH, Voss L, Böhmert L, Braeuning A, Sieg H. Uptake and cellular effects of PE, PP, PET and PVC microplastic particles. Toxicol in Vitro. 2021;70:105021. https://doi.org/10.1016/j.tiv.2020.105021.
38. Li B, Ding Y, Cheng X, Sheng D, Xu Z, Rong Q, Wu Y, Zhao H, Ji X, Zhang Y. Polyethylene microplastics affect the distribution of gut microbiota and inflammation development in mice. Chemosphere. 2020;244:125492. https://doi.org/10.1016/j.chemosphere.2019.125492.
39. Orsi M, Sanderson WE, Essex JW. Permeability of small molecules through a lipid bilayer: a multiscale simulation study. J Phys Chem B. 2009;113(35):12019–29. https://doi.org/10.1021/jp903248s.
40. Chen L, Chen J, Zhou G, Wang Y, Xu C, Wang X. Molecular Dynamics Simulations of the permeation of bisphenol A and pore formation in a lipid membrane. Sci Rep. 2016;6:33399. https://doi.org/10.1038/srep33399.
41. Hollóczki O, Gehrke S. Can nanoplastics alter cell membranes? ChemPhysChem. 2020;21(1):9–12. https://doi.org/10.1002/cphc.201900481.
42. Zhuang X, Makover JR, Im W, Klauda JB. A systematic molecular dynamics simulation study of temperature dependent bilayer structural properties. Biochim Biophys Acta. 2014;1838(10):2520–9. https://doi.org/10.1016/j.bbamem.2014.06.010.
43. Neale C, Pomès R. Sampling errors in free energy simulations of small molecules in lipid bilayers. Biochim Biophys Acta. 2016;1858(10):2539–48. https://doi.org/10.1016/j.bbamem.2016.03.006.
44. Frallicciardi J, Melcr J, Siginou P, Marrink SJ, Poolman B. Membrane thickness, lipid phase and sterol type are determining factors in the permeability of membranes to small solutes. Nat Commun. 2022;13:1605. https://doi.org/10.1038/s41467-022-29272-x.

Publisher's Note